



OPEN ACCESS

EDITED BY

Charles S. Via,
Uniformed Services University,
United States

REVIEWED BY

Ke Xu,
Shanxi Bethune Hospital, China
Vladimir Tesar,
Charles University, Czechia

*CORRESPONDENCE

Dimitrios Vassilopoulos
✉ dvassilop@med.uoa.gr

†These authors have contributed equally to this work

SPECIALTY SECTION

This article was submitted to Autoimmune and Autoinflammatory Disorders: Autoimmune Disorders, a section of the journal Frontiers in Immunology

RECEIVED 17 October 2022

ACCEPTED 13 March 2023

PUBLISHED 27 March 2023

CITATION

Banos A, Thomas K, Garantziotis P, Filia A, Malissovova N, Pieta A, Nikolakis D, Panagiotopoulos AG, Chalkia A, Petras D, Bertsias G, Boumpas DT and Vassilopoulos D (2023) The genomic landscape of ANCA-associated vasculitis: Distinct transcriptional signatures, molecular endotypes and comparison with systemic lupus erythematosus. *Front. Immunol.* 14:1072598. doi: 10.3389/fimmu.2023.1072598

COPYRIGHT

© 2023 Banos, Thomas, Garantziotis, Filia, Malissovova, Pieta, Nikolakis, Panagiotopoulos, Chalkia, Petras, Bertsias, Boumpas and Vassilopoulos. This is an open-access article distributed under the terms of the [Creative Commons Attribution License \(CC BY\)](https://creativecommons.org/licenses/by/4.0/). The use, distribution or reproduction in other forums is permitted, provided the original author(s) and the copyright owner(s) are credited and that the original publication in this journal is cited, in accordance with accepted academic practice. No use, distribution or reproduction is permitted which does not comply with these terms.

The genomic landscape of ANCA-associated vasculitis: Distinct transcriptional signatures, molecular endotypes and comparison with systemic lupus erythematosus

Aggelos Banos^{1†}, Konstantinos Thomas^{2†}, Panagiotis Garantziotis^{1,3†}, Anastasia Filia¹, Nikolaos Malissovova¹, Antigone Pieta^{1,4}, Dimitrios Nikolakis^{1,5,6,7}, Alexandros G. Panagiotopoulos², Aglaia Chalkia⁸, Dimitrios Petras⁸, George Bertsias^{9,10}, Dimitrios T. Boumpas^{1,4,11†} and Dimitrios Vassilopoulos^{2,11*†}

¹Laboratory of Autoimmunity and Inflammation, Center for Clinical, Experimental Surgery and Translational Research, Biomedical Research Foundation of the Academy of Athens, Athens, Greece,

²Clinical Immunology- Rheumatology Unit, 2nd Department of Medicine and Laboratory, General Hospital of Athens Ippokrateio, School of Medicine, National and Kapodistrian University of Athens, Athens, Greece, ³Department Rheumatology and Immunology, Hannover Medical School, Hannover, Germany, ⁴Rheumatology and Clinical Immunology Unit, 4th Department of Internal Medicine, Attikon University Hospital, Athens, Greece, ⁵Amsterdam Institute for Gastroenterology Endocrinology and Metabolism, Department of Gastroenterology, Academic Medical Center, Amsterdam University Medical Centers (UMC), University of Amsterdam, Amsterdam, Netherlands,

⁶Department of Rheumatology and Clinical Immunology, Amsterdam Rheumatology & Immunology Center (ARC), Amsterdam University Medical Centers (UMC), University of Amsterdam, Amsterdam, Netherlands, ⁷Amsterdam Institute for Infection & Immunity, Department of Experimental Immunology, Amsterdam University Medical Centers (UMC), University of Amsterdam, Amsterdam, Netherlands, ⁸Nephrology Department, General Hospital of Athens Ippokrateio, Athens, Greece, ⁹Department of Rheumatology and Clinical Immunology, University Hospital of Heraklion, Medical School, University of Crete, Heraklion, Greece, ¹⁰Department of Immunity, Institute of Molecular Biology and Biotechnology-Foundation of Research and Technology-Hellas (FORTH), Heraklion, Greece, ¹¹Joint Academic Rheumatology Program, School of Medicine, National and Kapodistrian University of Athens, Athens, Greece

Introduction: Anti-neutrophil cytoplasmic antibody (ANCA)-associated vasculitides (AAVs) present with a complex phenotype and are associated with high mortality and multi-organ involvement. We sought to define the transcriptional landscape and molecular endotypes of AAVs and compare it to systemic lupus erythematosus (SLE).

Methods: We performed whole blood mRNA sequencing from 30 patients with AAV (granulomatosis with polyangiitis/GPA and microscopic polyangiitis/MPA) combined with functional enrichment and network analysis for aberrant pathways. Key genes and pathways were validated in an independent cohort of 18 AAV patients. Co-expression network and hierarchical clustering analysis, identified molecular endotypes. Multi-level transcriptional overlap analysis to SLE was based on our published data from 142 patients.

Results: We report here that “Pan-vasculitis” signature contained 1,982 differentially expressed genes, enriched in leukocyte differentiation, cytokine signaling, type I and type II IFN signaling and aberrant B-T cell immunity. Active disease was characterized by signatures linked to cell cycle checkpoints and metabolism pathways, whereas ANCA-positive patients exhibited a humoral immunity transcriptional fingerprint. Differential expression analysis of GPA and MPA yielded an IFN- γ pathway (in addition to a type I IFN) in the former and aberrant expression of genes related to autophagy and mRNA splicing in the latter. Unsupervised molecular taxonomy analysis revealed four endotypes with neutrophil degranulation, aberrant metabolism and B-cell responses as potential mechanistic drivers. Transcriptional perturbations and molecular heterogeneity were more pronounced in SLE. Molecular analysis and data-driven clustering of AAV uncovered distinct transcriptional pathways that could be exploited for targeted therapy.

Discussion: We conclude that transcriptomic analysis of AAV reveals distinct endotypes and molecular pathways that could be targeted for therapy. The AAV transcriptome is more homogenous and less fragmented compared to the SLE which may account for its superior rates of response to therapy.

KEYWORDS

autoimmune diseases, vasculitis, lupus (SLE), transcriptomics (RNA-seq), endotypes of disease

Introduction

Anti-neutrophil cytoplasmic antibody (ANCA)-associated vasculitides (AAVs) include granulomatosis with polyangiitis (GPA), microscopic polyangiitis (MPA) and eosinophilic granulomatosis with polyangiitis (EGPA). They are associated with significant mortality (25% at five years after diagnosis) (1) and morbidity, due to disease- and treatment-related organ damage (2). AAV display a diverse clinical phenotype with multi-organ involvement including kidneys, upper and lower respiratory tract, nerves, joints, skin and the central nervous system. The organ involvement shows significant variation between patients and phenotypes, with 80% of renal-limited glomerulonephritis cases being positive for ANCA against myeloperoxidase (MPO+) and 90% of patients with ear, nose and throat involvement being positive for ANCA against proteinase-3 (PR3+) (3). Following induction therapy, more than 85% of patients will enter remission, however up to 40-50% of patients experience disease relapses despite maintenance immunosuppressive therapies (4). Given the complexity of the AAV natural course, the in-depth description of disease endotypes and the discovery of biomarkers to predict resistance to therapy, relapses or severe outcomes has become of paramount importance. To date, several candidate biomarkers have been tested for this purpose (i.e. B-cell count, ANCA type and titers) in randomized and observational trials, however most of them have come up with variable results (5–8). This better understanding of the underlying mechanisms of the disease has led to the introduction of novel therapies, such as those blocking the C5a receptor (avacopan) for AAV (9) and the anti-IFN I receptor (anifrolumab) for SLE.

AAV develop in genetically predisposed individuals following exposure to certain environmental factors (10). Genome-wide association studies (GWAS) have pointed to several major histocompatibility complex class II (MHC II) (11–13) and non-MHC (11, 12, 14) genes associated with AAV risk. Epigenetic mechanisms including DNA methylation, histone modification and therefore, expression regulation of key genes such as MPO and PRTN3 have also been described (15, 16). An interplay of several immune system components contributes to its pathogenesis, namely innate (neutrophil priming and activation, neutrophil extracellular traps (NETs) (17), alternative complement pathway) and adaptive immunity (CD4-induced B-cell stimulation and ANCA production by plasma cells, T helper 17 (Th17) cells forming and maintaining necrotizing granuloma, and finally quantitative and functional alteration of regulatory T cells (10, 18).

High throughput genomic technologies allow the systematic, comprehensive exploration of complex diseases without preconceived notions (19). Recently, using next-generation RNA sequencing we have defined signatures correlated with susceptibility, activity and severity in patients with systemic lupus erythematosus (SLE) and defined molecular endotypes of the disease (20). Different gene expression modules in SLE have been correlated with different clinical aspects. For example, CD4 and CD8 signatures were associated with disease outcome, whereas type 1 interferon response with disease activity (21). In AAVs, initial transcriptomic analyses revealed enrichment of genes implicated in IL7R pathway, TCR signaling and expansion of CD8 memory cells were associated with poor prognosis and higher relapse rates, whereas a distinct CD8 T-cell exhaustion signature correlated

with low risk of relapse (21, 22). More recently, RNA sequencing approaches have offered additional insights suggesting a strong neutrophilic and lymphocyte signature (23, 24) some of them reminiscent of those in SLE. Yet, despite its aggressive course, in AAV responses to existing therapies are more solid than those in SLE. Comparison of the transcriptomic landscape of both diseases provide an unbiased look of the underlying pathogenetic mechanisms and explain the differences in the natural course and response to treatment.

Herein, we sought to define the transcriptomic signature of AAV patients, identify potential differences in RNA signatures between AAV subsets, define novel molecular endotypes, and compare its transcriptome to that of SLE.

Materials and methods

Patients

Thirty adult patients with AAV (GPA or MPA) followed in two tertiary referral hospitals (Hippokraton General Hospital, HGH and Attikon University Hospital, AUH) were included. All patients fulfilled the Chapel Hill Consensus Conference definitions for GPA and MPA (25). Patients with EGPA were excluded due to its distinct pathogenesis and phenotype, in order to achieve a more homogenous cohort. The control group included 11 age- and sex-

matched healthy individuals. All participants provided informed consent. The study was approved by the institutional review boards of both hospitals (HGH: 57/26-03-2018/AUH: 103/06-03-2014).

For each patient, the following data were collected: age at diagnosis and at sampling, sex, type of AAV (GPA/MPA) and ANCA status, Birmingham Vasculitis Activity Score for Wegener's Granulomatosis (BVAS/WG) at diagnosis and at sampling, disease status at the time of sampling (active vs. remission), organ involvement, type of treatment at the time of blood sampling and, glucocorticoid dose (as prednisolone equivalent, mg/day). Active disease was defined as BVAS/WG >1. Disease remission was defined as BVAS/WG ≤ 1 for ≥6 months and daily prednisone dose of ≤10 mg (26). Relapse was defined as an at least 1-point increase in BVAS/WG in a patient previously in remission. Values are presented as mean ± standard deviation (SD) for continuous variables with normal distribution, median (interquartile range, IQR) for continuous nonparametric variables, and percentages for categorical variables (see Table 1).

Isolation of total RNA

Whole blood samples were collected in PaxGene and Tempus RNA tubes. Total RNA was extracted using the Qiagen RNeasy kit and quantification was assessed using a NanoDrop spectrometer. Quality control of RNA was assessed using the Agilent Bio Analyser.

TABLE 1 Demographics, clinical characteristics, and treatment at sampling of the 30 (discovery cohort) and 18 (validation cohort) AAV patients.

Variables	n (%)		p
	Discovery cohort n = 30	Validation cohort n = 18	
Males, n (%)	16 (53.3%)	8 (44.4%)	0.56
Age at diagnosis, mean (SD)	56.9 (14.9)	55.7 (17.7)	0.79
Age at sampling, mean (SD)	60.5 (14.1)	63.6 (17.2)	0.49
AAV type, n (%)			0.37
GPA	22 (73.3%)	11 (61.2%)	
MPA	8 (26.7%)	7 (38.8%)	
ANCA status, n (%)			0.49
cANCA/anti-PR3+	11 (36.7%)	9 (50.0%)	
pANCA/anti-MPO+	15 (50%)	8 (44.4%)	
Negative	4 (13.3%)	1 (5.6%)	
BVAS/WG at diagnosis, median (IQR)	6 (4-8)	5 (4-8.25)	0.76
BVAS/WG at sampling, median (IQR)	1 0 (4.25)	1 (0-2.75)	0.70
Organ involvement, n (%)			
Constitutional	18 (60%)	9 (50%)	0.49
Lung	27 (90%)	14 (77.8%)	0.24
Renal	21 (70%)	8 (44.4%)	0.08
ENT	15 (50%)	10 (55.5%)	0.71

(Continued)

TABLE 1 Continued

Variables	n (%)		p
	Discovery cohort n = 30	Validation cohort n = 18	
Mucous/Eyes/Membranes	4 (13.3%)	3 (16.7%)	0.75
Nervous	5 (16.7%)	7 (38.9%)	0.08
Cutaneous	3 (10%)	3 (16.7%)	0.49
Cardiovascular	1 (3.3%)	1 (5.6%)	0.99
Disease status at sampling, n (%)			0.32
Remission	13 (43.3%)	11 (61.1%)	
Active, newly diagnosed	8 (26.7%)	1 (5.6%)	
Active relapse	7 (23.3%)	5 (27.7%)	
Active, persistent	2 (6.7%)	1 (5.6%)	
Treatment type at sampling, n (%)			
No treatment	5 (16.7%)	5 (16.7%)	0.36
Corticosteroids	20 (66.7%)	10 (55.5%)	0.44
Cyclophosphamide	7 (23.3%)	0 (0%)	–
Rituximab	10 (33.3%)	8 (44.4%)	0.44
Azathioprine	9 (30%)	1 (5.5%)	0.09
Methotrexate	5 (16.7%)	0 (0%)	–
Mycophenolate mofetil	2 (6.7%)	2 (11.1%)	0.96
Prednisone dose at sampling, median (IQR)	3 (0-7.5)	3.75 (0-5)	0.85

Disease remission was defined as BVAS/WG ≤ 1 for ≥ 6 months and daily prednisone dose of ≤ 10 mg. Relapse was defined as an at least 1-point increase in BVAS/WG in a patient previously in remission. BVAS/WG, Birmingham Vasculitis Activity Score for Wegener's Granulomatosis; SD, standard deviation (SD); IQR interquartile range, IQR.

Library preparations and next-generation sequencing

mRNA libraries were prepared using the Illumina TruSeq kit. 1x75bp single-end mRNA sequencing was performed on the Illumina NextSeq 500 in the BRFAA Greek Genome Center.

Computational analysis of RNA sequencing data

Quality of sequencing was assessed using FastQC software (27). Raw reads in fastq format were aligned to the human reference genome (GRCh38.p12) by STAR mapper (28) and gene quantification was performed by HTSeq (29) using Gencode v29 annotation. Differential expression analysis was conducted using edgeR Bioconductor R package (quasi-likelihood linear model) (30). Statistically significant differentially expressed genes were considered those with a p-value of ≤ 0.05 and absolute fold change of ≥ 1.5 . Clustering of genes was performed using euclidean distance. Differential expressed genes for SLE analysis were extracted from published data as lists (20).

Enrichment analysis of DEGs and visualization were carried out using gProfiler (31), Enrichment Map (32), R Bioconductor packages, DOSE (33) and ReactomePA (34) and GeneMANIA (35) and GSEA (36). For all statistical comparisons, the cut-off for significance was set to 0.05 and p-values were adjusted for multiple comparisons.

Regulatory networks from the identified transcriptional signatures were constructed by applying the X2K Web algorithm (37), which creates a comprehensive network by integrating results from transcription factor enrichment analysis, protein-protein interaction network analysis, and kinase enrichment analysis (KEA) (38).

Co-expression network analysis

Using the CoCena² (construction of co-expression network analysis-automated, <https://github.com/UlasThomas/CoCena2>), we identified modules of co-expressed transcripts. Disease molecular endotypes were determined using agglomerative hierarchical clustering of patients, based on their group fold changes (GFC) for each cluster of co-expressed genes. Enrichment analysis was performed using the clusterProfilerR package (39).

qPCR validation

We performed qPCR for literature-curated genes as well as genes derived from gene ontology in an independent cohort of 18 AAV patients. Primer list is included as [Supplementary Table 1](#).

Results

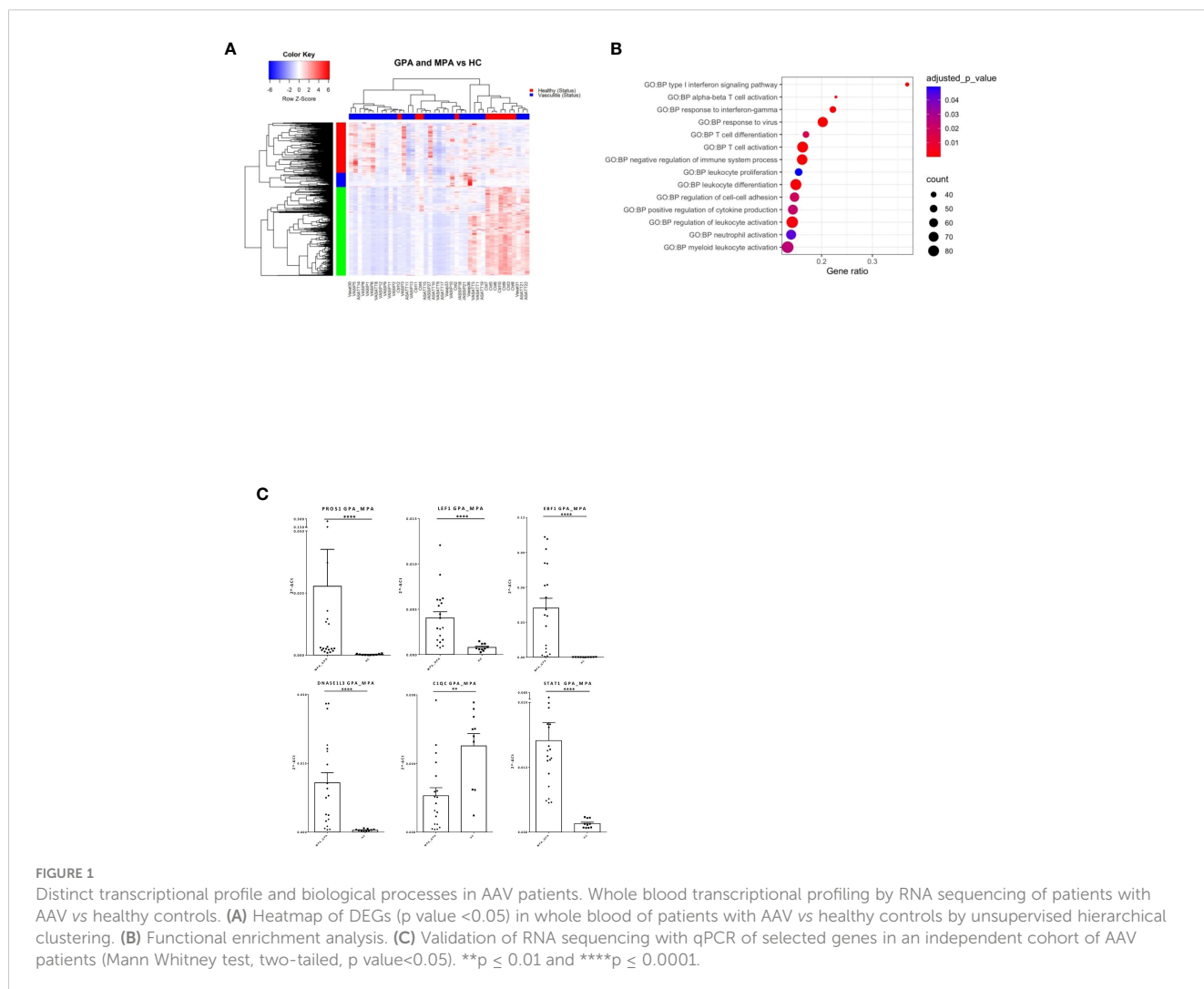
Patients

Thirty (30) AAV patients were included; 53.3% (16/30) were males, with a mean (\pm SD) age of 60.5 ± 14.1 years at the time of sampling. GPA was the most frequent clinical phenotype (22/30, 73.3%) whereas regarding ANCA status, 15 (50%) patients were pANCA/anti-MPO+, 11 (36.7%) were cANCA/anti-PR3+ and 4 (13.3%) were ANCA negative. Lung (90%), kidney (70%) and ENT (50%) were the more commonly affected organs. Thirteen (43%)

patients were in remission. Patient, disease and treatment characteristics are presented in [Table 1](#).

Cytokine signaling and B-cell and T-cell abnormal function differentiate AAV patients from healthy individuals

AAV comprise of various clinical phenotypes but a detailed molecular map of their common molecular basis is yet to be defined. Comparison of the blood transcriptomes of AAV patients versus healthy controls revealed a “pan-vasculitis” signature comprising 1,982 differentially expressed genes (DEGs) ([Figure 1A](#); [Supplementary Table 2](#)). DEGs related to neutrophil degranulation, type I interferon (IFN) signaling and aberrant T-cell responses were overrepresented in gene ontology analysis ([Figure 1B](#)). To validate our findings, qPCR was performed in an independent cohort of AAV and healthy individuals. Transcription



factors such as STAT1, EBF1, LEF1 and immune/complement related genes such as PROS1 and C1QC are among the validated genes (Figure 1C).

GPA is characterized by aberrant type I interferon and neutrophil degranulation gene signatures

To define GPA-specific gene signatures, the transcriptome of GPA patients was compared with that of matched healthy individuals yielding 1,319 DEGs (Figure 2A; Supplementary Table 3). Pathways involved in type I IFN and IFN- γ signaling as well as neutrophil mediated immune responses were extensively deregulated in GPA (Figure 2B). We identified IRF8, IRF1, STAT3, GATA1, GATA2 as putative upstream regulators of the GPA signature (Supplementary Figure 1A).

Unsupervised hierarchical clustering revealed four patterns of expression among DEGs. In addition to the aforementioned perturbations, enrichment analysis of a 222-gene cluster

underscored IL1b mediated responses in GPA pathogenesis (Supplementary Table 4). Interestingly, gene network representation of the 222-gene cluster identified genes related to IFN signaling, such as STAT1, ISG15, IFIT3, IFITM1, TRIM22 and histocompatibility genes, such as HLA-E, HLA-F as hub genes (Supplementary Figure 1B). qPCR of key genes in the independent patient and healthy cohorts resulted in validation of immune-related (FCRLA, MMP28, DNASE1L3) and developmental genes (PAX5) (Figure 2C).

These data suggest that broad type 1 IFN, IFN- γ and innate immunity deregulations may contribute to GPA initiation and progression.

MPA is characterized by transcriptome aberrations related to neutrophil degranulation, autophagy and mRNA splicing

Next, we characterized the transcriptome of MPA patients. A total of 2,326 DEGs were detected (Figure 3A; Supplementary

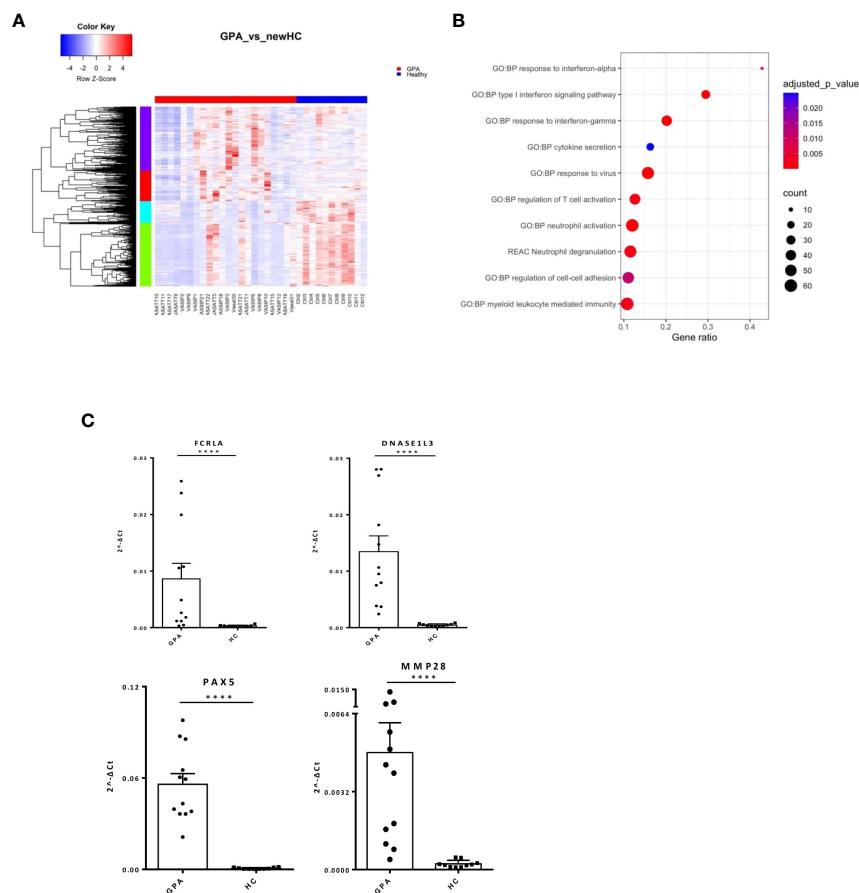
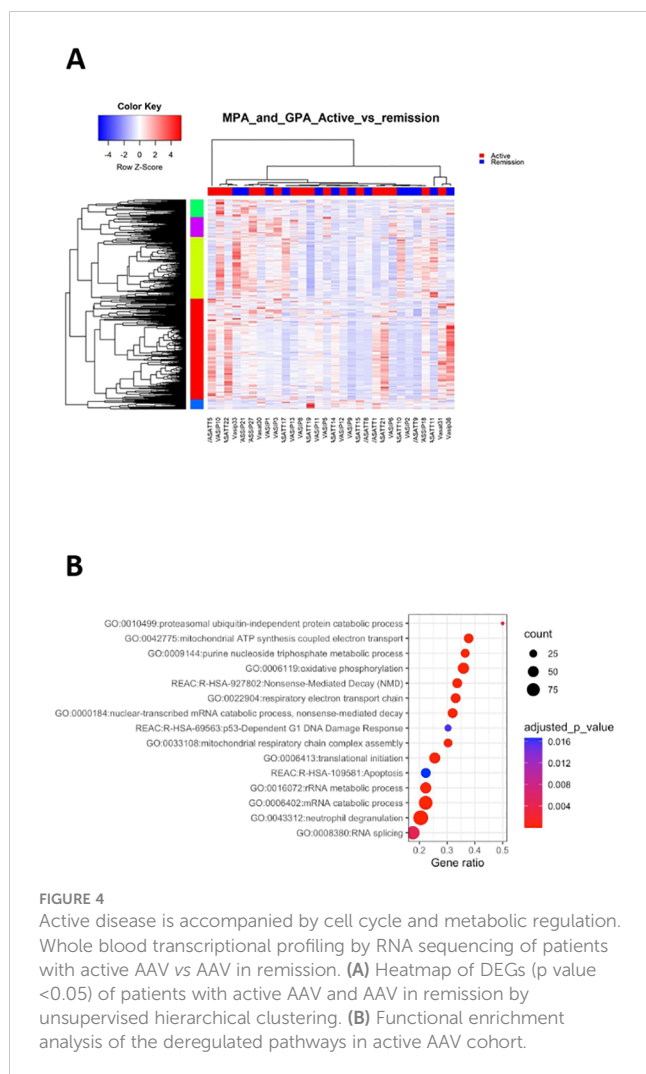


FIGURE 2 Neutrophil degranulation and type I IFN signaling characterize the GPA transcriptional map. Whole blood transcriptional profiling by RNA sequencing of patients with GPA vs healthy controls. **(A)** Heatmap of DEGs (p value < 0.05) in whole blood of patients with GPA and healthy controls by unsupervised hierarchical clustering. **(B)** Functional enrichment analysis of the deregulated pathways in GPA. **(C)** Validation of RNA sequencing with qPCR of selected genes in an independent cohort of GPA patients (Mann Whitney test, two-tailed, p value < 0.05). ****p ≤ 0.0001.



transcription factors including ELF1, CREB1, FLI1, MYC, NFYB, PML were detected (Supplementary Table 9). Interestingly, impaired expression of FLI1 has been implicated with other autoimmune disorders, such as SLE (45), whereas the CREB transcription factor family plays a role in the development and maintenance of Tregs (46). KEA returned 134 enriched kinases, including mitogen-activated protein kinase 1 (MAPK1), cyclin dependent kinase 4 (CDK4), homeodomain interacting protein kinase 2 (HIPK2) and Janus kinase 2 (JAK2) (Supplementary Table 10).

Together, deregulation of processes related to neutrophil degranulation, cell cycle progression and metabolism efficiently differentiated active disease, suggesting that restoration of their function might be linked with remission induction.

Humoral immunity gene expression signatures correlate with ANCA positivity

ANCA are implicated in AAV pathogenesis and furthermore, ANCA-positive patients display a different clinical course and response to therapies compared to ANCA-negative patients. Whether ANCA positivity is accompanied by specific

transcriptional signature remains elusive. By comparing the blood transcriptome of ANCA-positive with ANCA-negative patients, 182 DEGs were identified (Figure 5A; Supplementary Table 11). Pathways related to phagocytosis, activation of classical complement pathway, Fc-gamma receptor signaling and BCR activation were prominent in upregulated DEGs (Figure 5B). To determine genes with high impact on humoral immune responses, ranked GSEA and leading-edge analysis were performed (Figure 5C). Genes encoding constant and variable domains of immunoglobulin heavy chains, such as IGHE, IGHV3-23, IGLV7-43, IGLV7-43 contributed largely to the core enrichment.

To prioritize the upregulated DEGs, a GeneMANIA-based weighted interaction network was created (Supplementary Figure 3A). Highly interconnected nodes included, among others, genes essential for cytoskeleton organization and cell motility, such as ACTN4, MYH9, FLNA and TRRAP (47, 48). To capture a more detailed picture of the gene expression regulation, a X2K network corresponding to upregulated DEGs was constructed (Supplementary Figure 3B). Briefly, transcription factors, including GATA1, GATA2, SMAD4, NFE2L2, FOS were predicted to orchestrate gene activity.

GWAS analysis of patients with AAV shows that its pathogenesis has genetic component, distinguishing GPA from MPA as well as implying that PR3-AAV and MPO-AAV are distinct autoimmune syndromes, independent of the characteristics of the clinical phenotype (11). Therefore, this genetic impact on the phenotypes of AAV patients would probably be reflected on the respective transcriptomes. To address this question, we performed differential gene expression analysis based on the antibody specificity of the patients. MPO-ANCA positive transcriptomes (n=15) were compared to PR3-ANCA positive transcriptomes (n=11). Ultimately, 155 genes (104 upregulated) were differentially expressed between these two groups of patients (Supplementary Figure 4A, Supplemental Table 12). GSEA of the DEGs that dissect MPO+/PR3+ AAV patients pinpoints that they participate in complement activation, humoral immune response through circulating immunoglobulins, response to type I IFN, metabolism through oxidative phosphorylation and production of ROS (Supplementary Figure 4B; Supplemental Table 13).

Finally, we conclude that transcriptional signatures linked to aberrant humoral responses constitute a distinct characteristic of ANCA positive AAV. ANCA(+)*vs*(-) is discriminating molecular phenotype of the patients much more robustly than MPO(+)*vs*PR3(+).

Co-expression analysis revealed four AAV molecular endotypes with distinct gene expression signatures

Conventional differential expression analysis based on clinical classification often fails to fully explain molecular heterogeneity underlying immune responses in AAV. By contrast, co-expression analysis can facilitate a data-driven, clinically independent regrouping of samples. Using the CoCena² pipeline in our AAV

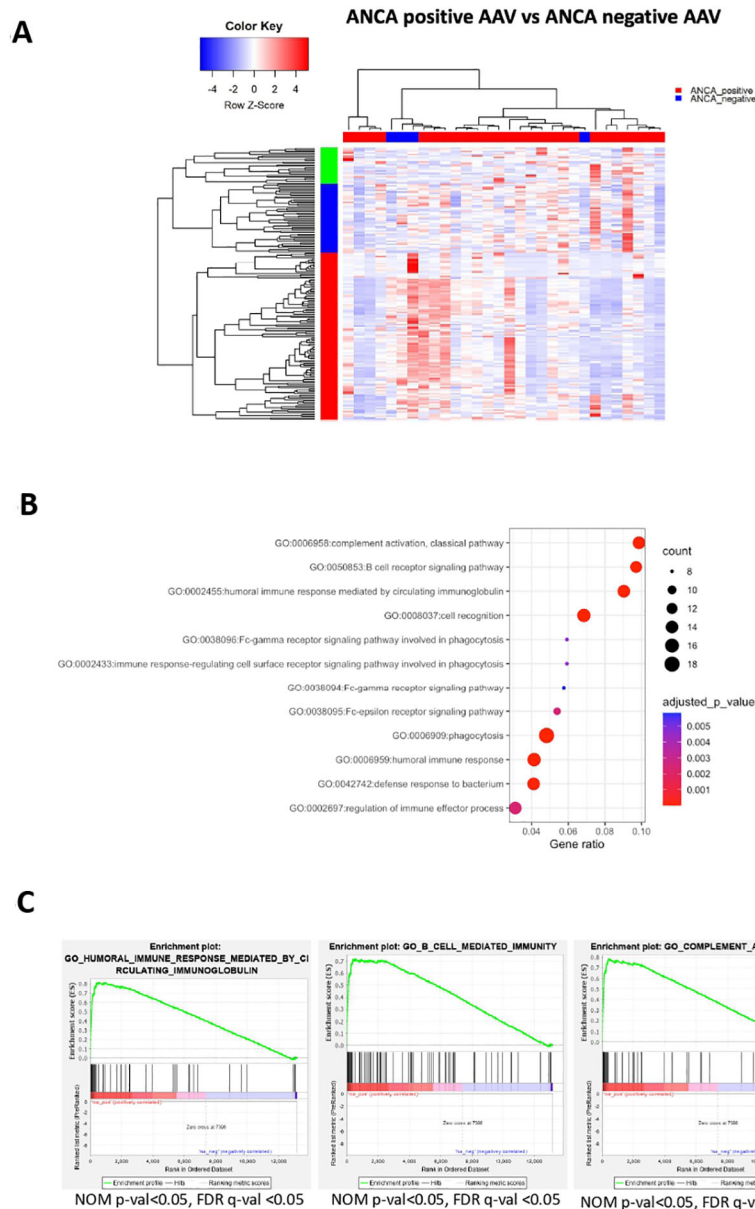


FIGURE 5 ANCA positivity is characterized by upregulation of genes related to humoral immunity. Whole blood transcriptional profiling by RNA sequencing of AAV patients according to their ANCA status **(A)** Heatmap of DEGs (p value < 0.05) of ANCA positive vs ANCA negative patients by unsupervised hierarchical clustering. **(B)** Functional enrichment analysis of the upregulated pathways in ANCA positive patients. **(C)** Ranked GSEA and leading-edge analysis to determine genes with high impact on humoral immune responses.

dataset, seven co-expression modules, which were represented by color dark grey to orchid were defined (Supplementary Figure 5A). Hierarchical clustering of the samples according to their group fold changes (GFCs) for each module, generated four groups of samples (G1-G4) (Figures 6A, B). To investigate the molecular basis of the applied re-stratification strategy, the enrichment of each newly defined group was examined (Figure 6C). Higher expression of orchid module, which contained genes involved in neutrophil degranulation, B cell mediated responses and complement activation distinguished G1 (Supplementary Figure 5B). G3, encompassing mainly patients with high BVAS score and upper respiratory tract involvement (Figure 6D), was characterized by

enrichment of the 131-gene erythropoiesis and platelet degranulation related dark orange module, along with dampening of the neutrophilic signature expression. Strikingly, genes of integrin family (ITGB3, ITGA2B, ITGB5), essential for neutrophil recruitment into inflamed tissues and phagocytosis were present in the dark orange module. The ANCA positive group G2, which was clinically discriminated by increased prevalence of pulmonary involvement, showed heightened expression of the dark green module. Detailed functionally enrichment analysis of the dark green module disclosed extensive deregulation of processes associated, among others, with oxidative phosphorylation and neutrophil activation.

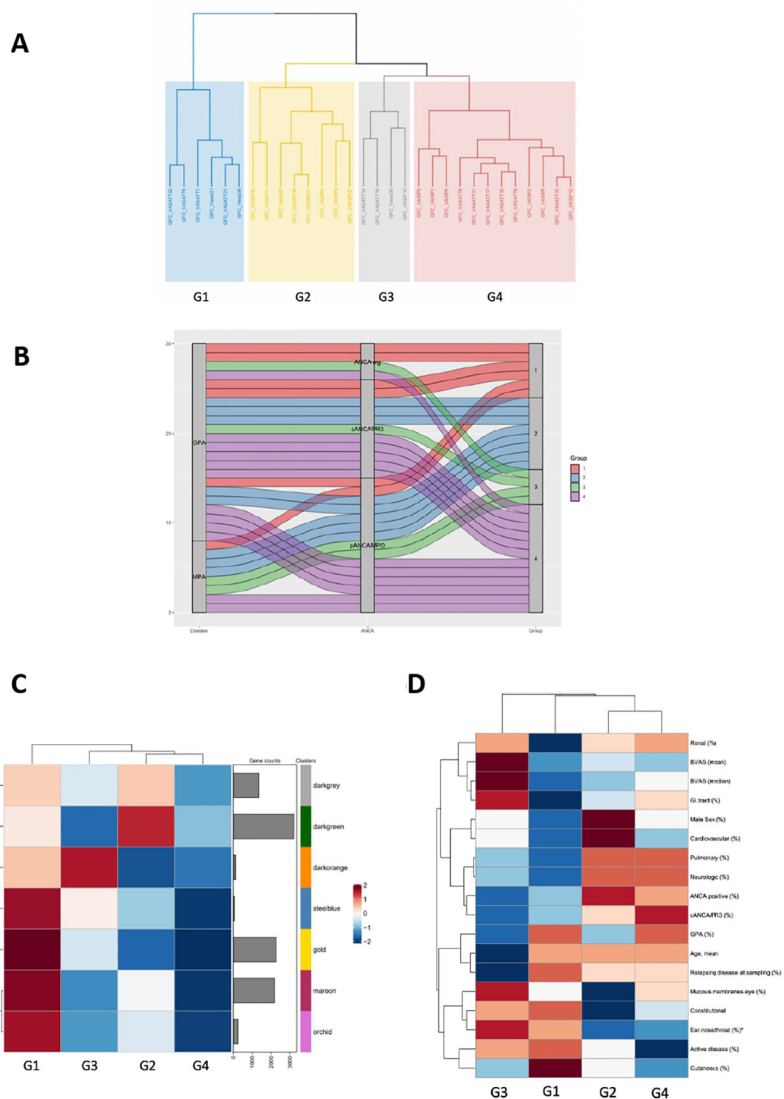


FIGURE 6
 Co-expression analysis of the AAV transcriptome defines distinct transcriptional modular patient clusters. **(A)** Hierarchical clustering of the samples according to their group fold changes (GFCs) for each module, generated four groups of samples (G1-G4). **(B)** Alluvial diagram showing the regrouping of patients according to co-expressed transcripts. **(C)** Heatmap demonstrating the mean of the GFCs of the gene modules – identified by the CoCena2 analysis – in each one of the defined patient groups. Enhanced expression of the orchid, maroon, gold and steelblue modules distinguished G1. Enrichment of the darkorange module characterized G3. Increased expression of the darkgreen module was indicative of G2. **(D)** Heatmap depicting the prevalence of the each AAV subtype, the distribution of the clinical and demographic features and the frequency of active disease across patient groups. *:p<0.05 in Kruskal-Wallis test, Chi-squared test.

Collectively, co-expression analysis suggested the presence of distinct AAV molecular endotypes.

Neutrophil and IFN-related pathways differences between SLE and AAV

Despite its aggressive course, in AAV responses to existing therapies are more solid than those in SLE. Comparison of the transcriptomic landscape of both diseases may provide an unbiased, comprehensive look of the underlying pathogenetic mechanisms and explain the differences in the natural course and response to treatment.

We investigated whether an overlap - in terms of DEGs and pathogenetic pathways – is present between SLE (20) and AAV (GPA or MPA). The comparison showed that 41%, 37% and 40% of the pathways derived of SLE DEGs, were also detected in the “Pan-vasculitis”, MPA and GPA gene expression signatures, respectively. (Figures 7A, B). GPA and SLE shared 199 enriched pathways (type I and II IFN signaling, neutrophil degranulation, cytokine signaling), whereas 207 biological processes were impaired both in SLE and MPA (metabolic pathways, autophagy, RNA metabolism and processing) (Figure 7B).

Since deregulations of neutrophils have emerged as a crucial driver of SLE and AAV pathogenesis (17, 49–52), we examined whether the neutrophil activation associated signatures qualitatively

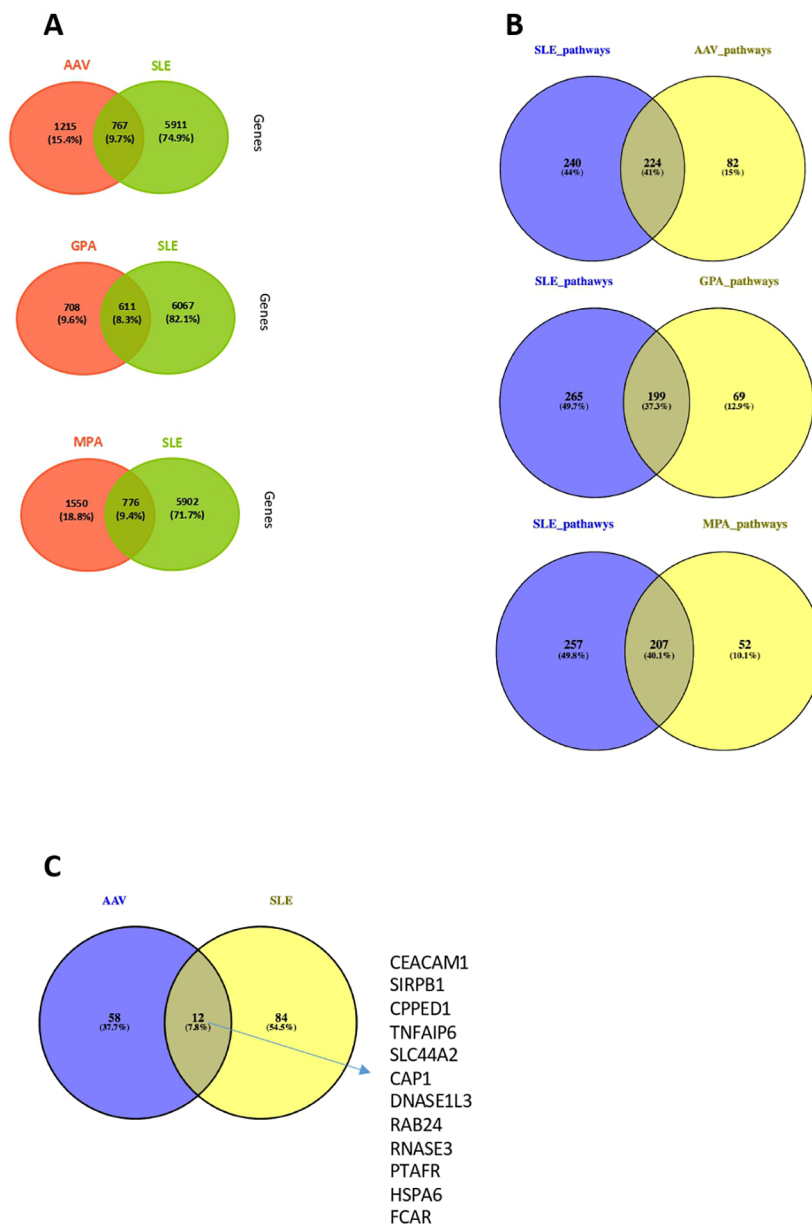


FIGURE 7 Comparison of whole blood transcriptome and neutrophil signature between AAV and SLE patients. **(A)** Venn diagrams representing the overlap between DEGs in AAV vs SLE, GPA vs SLE and MPA vs SLE. **(B)** Venn diagrams representing the overlap between involved pathways derived from gene ontology in AAV vs SLE, GPA vs SLE and MPA vs SLE. **(C)** Comparison at gene level between SLE and AAV neutrophilic signatures of these two gene sets.

differ between the two clinical entities. To this end, the DEGs belonging to the SLE neutrophilic signature were compared with the genes defining the AAV neutrophil signature. Of note, only a weak transcriptional overlap was observed between the SLE and AAV neutrophilic signatures, suggesting that distinct mechanisms underly neutrophilic inflammation in SLE and AAV (Figure 7C).

Discussion

Despite advances in the understanding of the molecular mechanisms underlying AAV, the disease etiopathogenesis

remains elusive. Herein, we identified aberrant IFN and neutrophil transcriptional responses associated with GPA and MPA. Deregulation of cell cycle checkpoints control, aberrancies of neutrophil function and cellular metabolism defined a status of active disease, while inappropriate humoral responses were related to ANCA positivity. By high-throughput computational methods, we re-stratified AAV patients based on their gene signatures, regardless of their clinical annotation. Finally, leveraging one of the largest SLE RNA sequencing cohort to date, we systematically explored the transcriptional similarities and differences between SLE and AAV, reporting more homogeneity and less “disorganization” in the AAV transcriptome.

Neutrophil activation and degranulation play a key role in AAV pathogenesis. ANCA-activated neutrophils generate ROS, release destructive enzymes and extrude NETs at the site of inflammation. Accordingly, augmented expression of the granulocyte gene signature is related to active disease and insufficient response to treatment (17, 49–52). Patients with active AAV displayed a robust transcriptomic neutrophilic signature. Low-density granulocytes (LDGs) – a distinct subset of neutrophils – exhibit increased capacity to form NETs (23, 53), suggesting that this cell type is likely to serve as a major source of the identified neutrophilic signature.

Necrotizing granuloma formation is a distinct feature of GPA. Interestingly, PR3-matured dendritic cells from GPA patients prime robust Th1 responses of PR3-specific CD4+ T cells, which in turn produce large amounts of IFN γ (54). It is tempting to speculate that enrichment of IFN γ related pathways in GPA blood transcriptome might account – at least in part – for the effect of PR3 on the functional maturation of dendritic cells.

Immunometabolism has emerged as a central mechanism for the regulation of adaptive and innate immune responses. In our study, patients with active disease exhibited disturbances of pathways involved in mitochondrial respiratory chain. Although neutrophils display limited reliance on oxidative phosphorylation at baseline, there is compelling evidence for the role of oxidative phosphorylation in NETosis and chemotaxis (55). The latter, coupled with the fact that excessive NET formation is present in active disease (17, 56) provides a reasonable interpretation of our findings.

Chronic inflammation favors genomic instability and DNA damage, setting DNA damage response and repair (DDR/R) in motion (57–60). Oxidative stress, characterized by excessive production and defective removal of ROS is a well-defined cause of DNA damage, leading to single-strand breaks, double-strand breaks and oxidized purines and pyrimidines (61). We are proposing that enrichment of cell cycle related pathways found in patients with active disease, might reflect a cellular response to DNA lesions, elicited by increased release of ROS by hyperactivated neutrophils (17, 49–52). Interestingly, genes related to type I IFN signature, including IRF3 were upregulated in active AAV, suggesting that accumulation of DNA lesions followed by induction of the cGAS-STING (stimulator of IFN genes)-IRF3 pathway and production of type I IFN (62) might be operant.

Clinical classification of AAV often fails to comprehensively recapitulate the mechanistic heterogeneity of the disease. Using co-expression network analysis, we re-grouped the AAV patients in an unbiased, data-driven manner. Neutrophil activation transcriptional signature defined G1, corroborating the molecular taxonomy findings of Gill et al. (24) Pathways reflecting neutrophil activation were not uniformly upregulated across the several endotypes, suggesting that additional mechanistic drivers might be present in AAV. Dysregulation of the mitochondrial function/oxidative phosphorylation dominated in patient group G2, whereas G3 demonstrated a transcriptional pattern indicative of platelet activation and erythropoiesis. Together, our data suggest that the transcriptome defined endotypes are not apparent with the current clinical classification or serologic status.

Defining gene expression signatures that differentiate AAV from SLE is fundamental for the development of accurate diagnostic biomarkers and might explain the differences in

response to therapy and risk of flares between these diseases. By applying an unsupervised, molecular taxonomy approach (20, 63), we have previously highlighted the broad heterogeneity, extensive fragmentation and wide reorganization of transcription in SLE (64). In contrast, the data-driven re-stratification of AAV demonstrated a significantly less extensive fragmentation of the AAV dataset. Although differences in sample size may affect our findings, a relative homogeneity of disease driving mechanisms in AAV, likely to favorably influence rates of response to treatment could be implied.

SLE and AAV are both characterized by a strong neutrophilic transcriptional signature. Interestingly, this signature exhibited important quantitative and qualitative differences between these diseases, suggesting that distinct pathophysiological mechanisms might orchestrate neutrophilic inflammation in SLE and AAV at different stages of the disease.

Our study has certain limitations. The vast majority of patients were receiving immunosuppressive treatment at sampling, including corticosteroids. Limitation associated with whole blood transcriptomic analysis, such as cellular heterogeneity should also be taken into consideration. As this study included only Caucasians, generalization of our results to other ethnic groups is questionable. We also recognize that the number of involved patients could be larger. However, our total cohort of AAV patients is similar to other prominent studies in the field. Second, the number of recruited patients is dependent on the AAV prevalence and, even though AAV are rare diseases, approximately one quarter of the AAV patients recruited in our multicenter registry were included in the current study. Third, the analytical power of RNA-sequencing can map both quantitative and qualitative dimensions of gene expression in an absolute statistically significant manner even with relatively limited number of patients. Of interest, while almost three out of four patients of our cohort had GPA, the respective prevalence of PR3, MPO and negative ANCA in this subset of patients was 50%, 32% and 18%. The subset of AAV patients with MPO-positive GPA is not uncommon and it has been reported in 16% of patients, while other observational studies have reported even higher prevalence (65–68). Given the relatively small number of included patients, we cannot rule out the possibility of a selection bias. Another limitation of this study is summed in the fact that no serial sampling were included so as to assess the disease trajectory as to activity and response to therapy. Finally, analysis of the transcriptome at the single cell level has added great amount of information about the pathogenic molecular landscape of various diseases, including autoimmune ones (69, 70). Single-cell studies in different vasculitides have already shed light on the pathogenesis of each entity, but for the time being they have focused on Takayasu arteritis (71), Behcet's Disease (72) and Kawasaki Disease (73, 74). Heterogeneity is analyzed in a certain degree in this study, as RNA-sequencing technology utilized is bulk.

In summary, our data provide a comprehensive assessment of the transcriptomic landscape of the human AAV in an unbiased way without preconceived notions, providing novel evidence for its key differences from the SLE transcriptome. In this context, we provide additional insights into the pathogenesis, monitoring and potential targets of therapy.

Data availability statement

Original datasets are available in a publicly accessible repository: The original contributions presented in the study are publicly available. The data presented in the study are deposited in the EGA repository, accession number EGAS00001006704, under the link <https://ega-archive.org/studies/EGAS00001006704>.

Ethics statement

The study was approved by the institutional review boards of 2 hospitals (HGH: 57/26-03-2018/AUH: EDB 103/06-03-2014). The patients/participants provided their written informed consent to participate in this study.

Author contributions

AB, KT and PG designed and performed the experiments, analysed data, generated figures and wrote the manuscript. AF, NM and DN analysed data and generated figures. NM performed experiments. KT, DP, AP, AC, AGP and PG performed clinical evaluation of patients, provided human specimens and interpreted data. GB participated in the design, the interpretation of data and the editing of the manuscript. DTB and DV supervised the study and the writing of the manuscript. AB, KT and PG contributed equally. DB and DV contributed equally. All authors contributed to the article and approved the submitted version.

Funding

This work was funded by the European Research Council under the European Union's Horizon 2020 research and innovation program (agreement no. 742390), by the Greek Rheumatology Society and Professional Association of Rheumatologists (ERE-EPERE), by the Special Account for Research Grants (S.A.R.G.), National and Kapodistrian University of Athens, Athens, Greece (DV, Grants #12085, 12086) and by SYSCID consortium (European Union's Horizon 2020 research and innovation programme under grant agreement No 733100). The research leading to these results has been co-funded by the European Commission under the H2020 Research Infrastructures contract no. 675121 (project VI-SEEM). Computational time was granted from the VI-SEEM project and the Greek national HPC facility—ARIS under project ID "RNA_LUPUS".

Acknowledgments

We thank Drs P. Katsimbri, A. Fanouriakis, S. Flouda, A. Chavatza, C. Tsalapaki, C. Koutsianas and nurses G. Rapsomaniki, K. Togia, A. Dourou and E. Mavrea for excellent patient care, as well as the patients for their participation in this study.

Conflict of interest

The authors declare that the research was conducted in the absence of any commercial or financial relationships that could be construed as a potential conflict of interest.

Publisher's note

All claims expressed in this article are solely those of the authors and do not necessarily represent those of their affiliated organizations, or those of the publisher, the editors and the reviewers. Any product that may be evaluated in this article, or claim that may be made by its manufacturer, is not guaranteed or endorsed by the publisher.

Supplementary material

The Supplementary Material for this article can be found online at: <https://www.frontiersin.org/articles/10.3389/fimmu.2023.1072598/full#supplementary-material>

SUPPLEMENTARY FIGURE 1

(A) Transcription factors predictive of regulating the GPA gene expression profile according to the ChIP Enrichment Analysis (ChEA). IRF1, STAT3 and GATA1 were identified as potential upstream regulators. (B) Gene network representation of a 222-gene cluster derived from the comparison of GPA with healthy individuals. Transcripts related to IFN signaling as well as histocompatibility genes emerged as hub genes.

SUPPLEMENTARY FIGURE 2

(A) Putative upstream regulators of the MPA signature according to the ChIP Enrichment Analysis (ChEA). Transcription factors associated with ribosomal RNA (rRNA) transcription, transcription initiation and epigenetic modifications were identified as essential regulators of the MPA transcriptional profile. (B) Enrichment map of the biological processes resulted from the functional enrichment analysis of a 101-gene cluster derived from the comparison of MPA with healthy individuals. Terms related to mRNA splicing were found – among others – to be significantly enriched. (C) Enrichment map of the biological processes resulted from the functional enrichment analysis of a 572-gene cluster derived from the comparison of MPA with healthy individuals. Pathways associated with neutrophil degranulation dominated in this gene-cluster. (D) Enrichment map of the biological processes resulted from the functional enrichment analysis of a gene cluster derived from the comparison of MPA with healthy individuals. Genes related to IFN responses were overrepresented among the DEGs of this gene cluster.

SUPPLEMENTARY FIGURE 3

(A) Gene network representation of the upregulated DEGs resulted from the comparison of ANCA positive patients with ANCA negative patients. Genes related to cytoskeleton organization and cell motility emerged as hub genes. (B) X2K Web based gene interaction network of the upregulated DEGs resulted from the comparison of ANCA positive patients with ANCA negative patients, inferred using the findings from transcription factor enrichment analysis, protein-protein interaction network analysis, and kinase enrichment analysis. Transcription factors, including GATA1, GATA2, SMAD4, NFE2L2, FOS were identified as potential regulators of the upregulated DEGs.

SUPPLEMENTARY FIGURE 4

(A) Heatmap of DEGs (p value <0.05) of anti-MPO+ve vs anti-PR3+ve patients by unsupervised hierarchical clustering. (B) Ranked GSEA resulted from the comparison of the whole blood transcriptome of anti-MPO+ve versus anti-PR3+ve patients.

SUPPLEMENTARY FIGURE 5

(A) CoCena2 analysis-based modules (darkgrey to orchid) of commonly regulated transcripts and heatmap demonstrating the group fold changes (GFC) of each sample per module. GFCs of each sample per module were calculated as previously described in Garantziotis et al. [58]. (B) Functional enrichment analysis of the CoCena2 analysis derived modules. Briefly, transcripts included in the orchid module were mainly enriched in processes related to neutrophil degranulation and B cell mediated responses. Enrichment analysis of the darkorange module revealed pathways associated with erythropoiesis and platelet degranulation. Genes of darkgreen module were enriched in oxidative phosphorylation and neutrophil activation.

SUPPLEMENTARY TABLE 1

Primer list used for the qPCR validation of the literature-curated genes.

SUPPLEMENTARY TABLE 2

Differentially expressed genes resulted from the comparison of the whole blood transcriptome of patients with GPA or MPA versus healthy individuals.

SUPPLEMENTARY TABLE 3

Differentially expressed genes resulted from the comparison of the whole blood transcriptome of patients with GPA versus healthy individuals.

SUPPLEMENTARY TABLE 4

Functional enrichment analysis of the 222-gene cluster identified by the unsupervised hierarchical clustering of the DEGs derived from the comparison of patients with GPA versus healthy individuals.

SUPPLEMENTARY TABLE 5

Differentially expressed genes resulted from the comparison of the whole blood transcriptome of patients with MPA versus healthy individuals.

SUPPLEMENTARY TABLE 6

Kinases predictive of regulating the MPA gene expression signature according to the KEA.

SUPPLEMENTARY TABLE 7

Differentially expressed genes resulted from the comparison of the whole blood transcriptome of active AAV patients versus AAV patients in remission.

SUPPLEMENTARY TABLE 8

Functional enrichment analysis of the DEGs defining the active AAV gene expression signature.

SUPPLEMENTARY TABLE 9

Transcription factors predictive of regulating the active disease gene expression signature according to the X2K Web based transcription factor enrichment analysis.

SUPPLEMENTARY TABLE 10

Kinases predictive of regulating the active disease gene expression signature according to the KEA.

SUPPLEMENTARY TABLE 11

Differentially expressed genes resulted from the comparison of the whole blood transcriptome of ANCA-positive versus ANCA-negative patients.

SUPPLEMENTARY TABLE 12

Differentially expressed genes resulted from the comparison of the whole blood transcriptome of anti-MPO+ve versus anti-PR3+ve patients.

SUPPLEMENTARY TABLE 13

Ranked GSEA analysis resulted from the comparison of the whole blood transcriptome of anti-MPO+ve versus anti-PR3+ve patients.

References

- Flossmann O, Berden A, de Groot K, Hagen C, Harper L, Heijl C, et al. Long-term patient survival in ANCA-associated vasculitis. *Ann Rheum Dis* (2011) 70:488–94. doi: 10.1136/ard.2010.137778
- Robson J, Doll H, Suppiah R, Flossmann O, Harper L, Höglund P, et al. Damage in the anca-associated vasculitides: Long-term data from the European vasculitis study group (EUVAS) therapeutic trials. *Ann Rheum Dis* (2015) 74:177–84. doi: 10.1136/annrheumdis-2013-203927
- Jennette JC, Nachman PH. ANCA glomerulonephritis and vasculitis. *Clin J Am Soc Nephrol* (2017) 12:1680–91. doi: 10.2215/CJN.02500317
- Walsh M, Flossmann O, Berden A, Westman K, Höglund P, Stegeman C, et al. Risk factors for relapse of antineutrophil cytoplasmic antibody-associated vasculitis. *Arthritis Rheum* (2012) 64:542–8. doi: 10.1002/art.33361
- Kemna MJ, Damoiseaux J, Austen J, Winkens B, Peters J, van Paassen P, et al. ANCA as a predictor of relapse: Useful in patients with renal involvement but not in patients with nonrenal disease. *J Am Soc Nephrol* (2015) 26:537–42. doi: 10.1681/ASN.2013111233
- Fussner LA, Hummel AM, Schroeder DR, Silva F, Cartin-Ceba R, Snyder MR, et al. Factors determining the clinical utility of serial measurements of antineutrophil cytoplasmic antibodies targeting proteinase 3. *Arthritis Rheumatol* (2016) 68:1700–10. doi: 10.1002/art.39637
- Specks U, Merkel PA, Seo P, Spiera R, Langford CA, Hoffman GS, et al. Efficacy of remission-induction regimens for ANCA-associated vasculitis. *N Engl J Med* (2013) 369:417–27. doi: 10.1056/NEJMoa1213277
- Guillevin L, Pagnoux C, Karras A, Khouatra C, Aumaitre O, Cohen P, et al. Rituximab versus azathioprine for maintenance in ANCA-associated vasculitis. *N Engl J Med* (2014) 371:1771–80. doi: 10.1056/NEJMoa1404231
- Jayne DRW, Merkel PA, Schall TJ, Bekker PADVOCATE Study Group. Avacopan for the treatment of ANCA-associated vasculitis. *N Engl J Med* (2021) 384:599–609. doi: 10.1056/NEJMoa2023386
- Nakazawa D, Masuda S, Tomaru U, Ishizu A. Pathogenesis and therapeutic interventions for ANCA-associated vasculitis. *Nat Rev Rheumatol* (2019) 15:91–101. doi: 10.1038/s41584-018-0145-y
- Lyons PA, Rayner TF, Trivedi S, Holle JU, Watts RA, Jayne DR, et al. Genetically distinct subsets within ANCA-associated vasculitis. *New Engl J Med* (2012) 367:214–23. doi: 10.1056/NEJMoa1108735
- Xie G, Roshandel D, Sherva R, Monach PA, Lu EY, Kung T, et al. Association of granulomatosis with polyangiitis (Wegener's) with *HLA-DPB1*04* and *SEMA6A* gene variants: Evidence from genome-wide analysis. *Arthritis Rheum* (2013) 65:2457–68. doi: 10.1002/art.38036
- Kawasaki A, Hasebe N, Hidaka M, Hirano F, Sada KE, Kobayashi S, et al. Protective role of HLA-DRB1*13:02 against microscopic polyangiitis and MPO-ANCA-Positive vasculitides in a Japanese population: A case-control study. *PLoS One* (2016) 11:e0154393. doi: 10.1371/journal.pone.0154393
- Cao Y, Yang J, Colby K, Hogan SL, Hu Y, Jennette CE, et al. High basal activity of the PTPN22 gain-of-function variant blunts leukocyte responsiveness negatively affecting IL-10 production in ANCA vasculitis. *PLoS One* (2012) 7:e42783. doi: 10.1371/journal.pone.0042783
- Yang J, Ge H, Poulton CJ, Hogan SL, Hu Y, Jones BE, et al. Histone modification signature at myeloperoxidase and proteinase 3 in patients with anti-neutrophil cytoplasmic autoantibody-associated vasculitis. *Clin Epigenet* (2016) 8:85. doi: 10.1186/s13148-016-0251-0
- Jones BE, Yang J, Muthigi A, Hogan SL, Hu Y, Starmer J, et al. Gene-specific DNA methylation changes predict remission in patients with ANCA-associated vasculitis. *J Am Soc Nephrol* (2017) 28:1175–87. doi: 10.1681/ASN.2016050548
- Kambas K, Chrysanthopoulou A, Vassilopoulos D, Apostolidou E, Skendros P, Girod A, et al. Tissue factor expression in neutrophil extracellular traps and neutrophil derived microparticles in antineutrophil cytoplasmic antibody associated vasculitis may promote thromboinflammation and the thrombophilic state associated with the disease. *Ann Rheum Dis* (2014) 73:1854–63. doi: 10.1136/annrheumdis-2013-203430
- von Borstel A, Sanders JS, Rutgers A, Stegeman CA, Heeringa P, Abdulahad WH. Cellular immune regulation in the pathogenesis of ANCA-associated vasculitides. *Autoimmun Rev* (2018) 17:413–21. doi: 10.1016/j.autrev.2017.12.002
- Flint S, McKinney E, Lyons P, Smith KG. The contribution of transcriptomics to biomarker development in systemic vasculitis and SLE. *Curr Pharm Des* (2015) 21:2225–35. doi: 10.2174/1381612821666150313130256
- Panousis NI, Bertias GK, Ongen H, Gergianaki I, Tektonidou MG, Trachana M, et al. Combined genetic and transcriptome analysis of patients with SLE: distinct, targetable signatures for susceptibility and severity. *Ann Rheum Dis* (2019) 78:1079–89. doi: 10.1136/annrheumdis-2018-214379

21. McKinney EF, Lee JC, Jayne DR, Lyons PA, Smith KG. T-Cell exhaustion, co-stimulation and clinical outcome in autoimmunity and infection. *Nature* (2015) 523:612–6. doi: 10.1038/nature14468
22. McKinney EF, Lyons PA, Carr EJ, Hollis JL, Jayne DR, Willcocks LC, et al. A CD8+ T cell transcription signature predicts prognosis in autoimmune disease. *Nat Med* (2010) 16:586–91. doi: 10.1038/nm.2130
23. Grayson PC, Carmona-Rivera C, Xu L, Lim N, Gao Z, Asare AL, et al. Neutrophil-related gene expression and low-density granulocytes associated with disease activity and response to treatment in antineutrophil cytoplasmic antibody-associated vasculitis. *Arthritis Rheumatol* (2015) 67:1922–32. doi: 10.1002/art.39153
24. Gill EE, Smith ML, Gibson KM, Morishita KA, Lee AHY, Falsafi R, et al. Different disease endotypes in phenotypically similar vasculitides affecting small-to-Medium sized blood vessels. *Front Immunol* (2021) 12:638571. doi: 10.3389/fimmu.2021.638571
25. Jennette JC, Falk RJ, Bacon PA, Basu N, Cid MC, Ferrario F, et al. 2012 Revised international chapel hill consensus conference nomenclature of vasculitides. *Arthritis Rheum* (2013) 65:1–11. doi: 10.1002/art.37715
26. Ntatsaki E, Carruthers D, Chakravarty K, D'Cruz D, Harper L, Jayne D, et al. BSR and BHRP guideline for the management of adults with ANCA-associated vasculitis. *Rheumatology* (2014) 53:2306–9. doi: 10.1093/rheumatology/ket445
27. Andrews S. *FastQC a quality control tool for high throughput sequence data secondary*. Available at: <http://www.bioinformatics.babraham.ac.uk/projects/fastqc/>.
28. Dobin A, Davis CA, Schlesinger F, Drenkow J, Zaleski C, Jha S, et al. STAR: ultrafast universal RNA-seq aligner. *Bioinformatics* (2013) 29:15–21. doi: 10.1093/bioinformatics/bts635
29. Anders S, Pyl PT, Huber W. HTSeq—a Python framework to work with high-throughput sequencing data. *Bioinformatics* (2015) 31:166–9. doi: 10.1093/bioinformatics/btu638
30. Robinson MD, McCarthy DJ, Smyth GK. edgeR: a bioconductor package for differential expression analysis of digital gene expression data. *Bioinformatics* (2010) 26:139–40. doi: 10.1093/bioinformatics/btp616
31. Reimand J, Kull M, Peterson H, Hansen J, Vilo J. g:Profiler—a web-based toolset for functional profiling of gene lists from large-scale experiments. *Nucleic Acids Res* (2007) 35:W193–200. doi: 10.1093/nar/gkm226
32. Isserlin R, Merico D, Voisin V, Bader GD. Enrichment map—a cytoscape app to visualize and explore OMICS pathway enrichment results. *F1000Res* (2014) 3:141. doi: 10.12688/f1000research.4536.1
33. Yu G, Wang L-G, Yan G-R, He QY. DOSE: an R/Bioconductor package for disease ontology semantic and enrichment analysis. *Bioinformatics* (2015) 31:608–9. doi: 10.1093/bioinformatics/btu684
34. Yu G, He Q-Y. ReactomePA: an R/Bioconductor package for reactome pathway analysis and visualization. *Mol Biosyst* (2016) 12:477–9. doi: 10.1039/C5MB00663E
35. Warde-Farley D, Donaldson SL, Comes O, Zuberi K, Badrawi R, Chao P, et al. The GeneMANIA prediction server: Biological network integration for gene prioritization and predicting gene function. *Nucleic Acids Res* (2010) 38:W214–20. doi: 10.1093/nar/gkq537
36. Subramanian A, Tamayo P, Mootha VK, Mukherjee S, Ebert BL, Gillette MA, et al. Gene set enrichment analysis: A knowledge-based approach for interpreting genome-wide expression profiles. *Proc Natl Acad Sci* (2005) 102:15545–50. doi: 10.1073/pnas.0506580102
37. Chen EY, Xu H, Gordonov S, Lim MP, Perkins MH, Ma'ayan A. Expression2Kinases: mRNA profiling linked to multiple upstream regulatory layers. *Bioinformatics* (2012) 28:105–11. doi: 10.1093/bioinformatics/btr625
38. Lachmann A, Ma'ayan A. KEA: Kinase enrichment analysis. *Bioinformatics* (2009) 25:684–6. doi: 10.1093/bioinformatics/btp026
39. Yu G, Wang L-G, Han Y, He QY. clusterProfiler: An R package for comparing biological themes among gene clusters. *OMICS* (2012) 16:284–7. doi: 10.1089/omi.2011.0118
40. Devaiah BN, Lu H, Geggone A, Sercan Z, Zhang H, Clifford RJ, et al. Novel functions for TAF7, a regulator of TAF1-independent transcription. *J Biol Chem* (2010) 285:38772–80. doi: 10.1074/jbc.M110.173864
41. Gordon S, Akopyan G, Garban H, Bonavida B. Transcription factor YY1: structure, function, and therapeutic implications in cancer biology. *Oncogene* (2006) 25:1125–42. doi: 10.1038/sj.onc.1209080
42. Tsai M-H, Pai L-M, Lee C-K. Fine-tuning of type I interferon response by STAT3. *Front Immunol* (2019) 10:1448. doi: 10.3389/fimmu.2019.01448
43. Moiseeva TN, Bottrill A, Melino G, Barlev NA. DNA Damage-induced ubiquitylation of proteasome controls its proteolytic activity. *Oncotarget* (2013) 4:1338–48. doi: 10.18632/oncotarget.1060
44. Clarke DJB, Kuleshov MV, Schilder BM, Torre D, Duffy ME, Keenan AB, et al. eXpression2Kinases (X2K) web: linking expression signatures to upstream cell signaling networks. *Nucleic Acids Res* (2018) 46:W171–9. doi: 10.1093/nar/gky458
45. Li Y, Luo H, Liu T, Zacksenhaus E, Ben-David Y. The ets transcription factor fl-1 in development, cancer and disease. *Oncogene* (2015) 34:2022–31. doi: 10.1038/onc.2014.162
46. Wen AY, Sakamoto KM, Miller LS. The role of the transcription factor CREB in immune function. *J Immunol* (2010) 185:6413–9. doi: 10.4049/jimmunol.1001829
47. McMahon SB, van Buskirk HA, Dugan KA, Copeland TD, Cole MD. The novel ATM-related protein TRRAP is an essential cofactor for the c-myc and E2F oncoproteins. *Cell* (1998) 94:363–74. doi: 10.1016/S0092-8674(00)81479-8
48. Tapias A, Zhou Z-W, Shi Y, Chong Z, Wang P, Groth M, et al. Trapp-dependent histone acetylation specifically regulates cell-cycle gene transcription to control neural progenitor fate decisions. *Cell Stem Cell* (2014) 14:632–43. doi: 10.1016/j.stem.2014.04.001
49. Falk RJ, Terrell RS, Charles LA, Jennette JC. Anti-neutrophil cytoplasmic autoantibodies induce neutrophils to degranulate and produce oxygen radicals *in vitro*. *Proc Natl Acad Sci* (1990) 87:4115–9. doi: 10.1073/pnas.87.11.4115
50. Charles LA, Caldas MLR, Falk RJ, Terrell RS, Jennette JC. Antibodies against granule proteins activate neutrophils. *In Vitro J Leukoc Biol* (1991) 50:539–46. doi: 10.1002/jlb.50.6.539
51. Kessenbrock K, Krumbholz M, Schönemarker U, Back W, Gross WL, Werb Z, et al. Netting neutrophils in autoimmune small-vessel vasculitis. *Nat Med* (2009) 15:623–5. doi: 10.1038/nm.1959
52. Nakazawa D, Shida H, Kusunoki Y, Miyoshi A, Nishio S, Tomaru U, et al. The responses of macrophages in interaction with neutrophils that undergo NETosis. *J Autoimmun* (2016) 67:19–28. doi: 10.1016/j.jaut.2015.08.018
53. Carmona-Rivera C, Kaplan MJ. Low-density granulocytes: a distinct class of neutrophils in systemic autoimmunity. *Semin Immunopathol* (2013) 35:455–63. doi: 10.1007/s00281-013-0375-7
54. Csernok E, Ai M, Gross WL, Wicklein D, Petersen A, Lindner B, et al. Wegener autoantigen induces maturation of dendritic cells and licenses them for Th1 priming via the protease-activated receptor-2 pathway. *Blood* (2006) 107:4440–8. doi: 10.1182/blood-2005-05-1875
55. Rice CM, Davies LC, Subleski JJ, Maio N, Gonzalez-Cotto M, Andrews C, et al. Tumour-elicited neutrophils engage mitochondrial metabolism to circumvent nutrient limitations and maintain immune suppression. *Nat Commun* (2018) 9:5099. doi: 10.1038/s41467-018-07505-2
56. Kraaij T, Kamerling SWA, van Dam LS, Bakker JA, Bajema IM, Page T, et al. Excessive neutrophil extracellular trap formation in ANCA-associated vasculitis is independent of ANCA. *Kidney Int* (2018) 94:139–49. doi: 10.1016/j.kint.2018.01.013
57. Souliotis VL, Sfikakis PP. Increased DNA double-strand breaks and enhanced apoptosis in patients with lupus nephritis. *Lupus* (2015) 24:804–15. doi: 10.1177/0961203314565413
58. Souliotis VL, Vlachogiannis NI, Pappa M, Argyriou A, Sfikakis PP. DNA Damage accumulation, defective chromatin organization and deficient DNA repair capacity in patients with rheumatoid arthritis. *Clin Immunol* (2019) 203:28–36. doi: 10.1016/j.clim.2019.03.009
59. Shao W-H, Cohen PL. Disturbances of apoptotic cell clearance in systemic lupus erythematosus. *Arthritis Res Ther* (2010) 13:202. doi: 10.1186/ar3206
60. Palomino GM, Bassi CL, Wastowski IJ, Xavier DJ, Lucisano-Valim YM, Crispim JC, et al. Patients with systemic sclerosis present increased DNA damage differentially associated with DNA repair gene polymorphisms. *J Rheumatol* (2014) 41:458–65. doi: 10.3899/jrheum.130376
61. Bokhari B, Sharma S. Stress marks on the genome: Use or lose? *Int J Mol Sci* (2019) 20:364. doi: 10.3390/ijms20020364
62. Härtlova A, Erttmann SF, Raffi FA, Schmalz AM, Resch U, Anugula S, et al. DNA Damage primes the type I interferon system via the cytosolic DNA sensor STING to promote anti-microbial innate immunity. *Immunity* (2015) 42:332–43. doi: 10.1016/j.immuni.2015.01.012
63. Garantziotis P, Nikolakis D, Doumas S, Frangou E, Sentsis G, Filia A, et al. Molecular taxonomy of systemic lupus erythematosus through data-driven patient stratification: Molecular endotypes and cluster-tailored drugs. *Front Immunol* (2022) 13:860726. doi: 10.3389/fimmu.2022.860726
64. Ntasis VF, Panousis NI, Tektonidou MG, Dermizakis ET, Boumpas DT, Bertias GK, et al. Extensive fragmentation and re-organization of transcription in systemic lupus erythematosus. *Sci Rep* (2020) 10:16648. doi: 10.1038/s41598-020-73654-4
65. Puéchal X, Iudici M, Pagnoux C, Cohen P, Hamidou M, Aouba A, et al. Comparative study of granulomatosis with polyangiitis subsets according to ANCA status: data from the French vasculitis study group registry. *RMD Open* (2022) 8. doi: 10.1136/rmdopen-2021-002160
66. Milosavlsky EM, Lu N, Unizony S, Choi HK, Merkel PA, Seo P, et al. Myeloperoxidase-antineutrophil cytoplasmic antibody (ANCA)-positive and ANCA-negative patients with granulomatosis with polyangiitis (Wegener's): Distinct patient subsets. *Arthritis Rheumatol* (2016) 68:2945–52. doi: 10.1002/art.39812
67. Chang D-Y, Li Z-Y, Chen M, Zhao MH. Myeloperoxidase-ANCA-positive granulomatosis with polyangiitis is a distinct subset of ANCA-associated vasculitis: A retrospective analysis of 455 patients from a single center in China. *Semin Arthritis Rheum* (2019) 48:701–6. doi: 10.1016/j.semarthrit.2018.05.003

68. Schirmer JH, Wright MN, Herrmann K, Laudien M, Nölle B, Reinhold-Keller E, et al. Myeloperoxidase-antineutrophil cytoplasmic antibody (ANCA)-positive granulomatosis with polyangiitis (Wegener's) is a clinically distinct subset of ANCA-associated vasculitis: A retrospective analysis of 315 patients from a German vasculitis referral center. *Arthritis Rheumatol* (2016) 68:2953–63. doi: 10.1002/art.39786
69. Perez RK, Gordon MG, Subramaniam M, Kim MC, Hartoularos GC, Targ S, et al. Single-cell RNA-seq reveals cell type-specific molecular and genetic associations to lupus. *Sci (1979)* (2022) 376. doi: 10.1126/science.abf1970
70. Zhang F, Wei K, Slowikowski K, Fonseka CY, Rao DA, Kelly S, et al. Defining inflammatory cell states in rheumatoid arthritis joint synovial tissues by integrating single-cell transcriptomics and mass cytometry. *Nat Immunol* (2019) 20:928–42. doi: 10.1038/s41590-019-0378-1
71. Qing G, Zhiyuan W, Jinge Y, Yuqing M, Zuoguan C, Yongpeng D, et al. Single-cell RNA sequencing revealed CD14+ monocytes increased in patients with takayasu's arteritis requiring surgical management. *Front Cell Dev Biol* (2021) 9:761300. doi: 10.3389/fcell.2021.761300
72. Zheng W, Wang X, Liu J, Yu X, Li L, Wang H, et al. Single-cell analyses highlight the proinflammatory contribution of C1q-high monocytes to behçet's disease. *Proc Natl Acad Sci* (2022) 119. doi: 10.1073/pnas.2204289119
73. Wang Z, Xie L, Ding G, Song S, Chen L, Li G, et al. Single-cell RNA sequencing of peripheral blood mononuclear cells from acute Kawasaki disease patients. *Nat Commun* (2021) 12:5444. doi: 10.1038/s41467-021-25771-5
74. Porritt RA, Zemmour D, Abe M, Lee Y, Narayanan M, Carvalho TT, et al. NLRP3 inflammasome mediates immune-stromal interactions in vasculitis. *Circ Res* (2021) 129:e183–e200. doi: 10.1161/CIRCRESAHA.121.319153